# Prediction of material damping of laminated polymer matrix composites

C. T. SUN, J. K. WU
*Department of Engineering Sciences, University of Florida, Gainesville, Florida 32611, USA*
R. F. GIBSON
*Department of Mechanical Engineering, University of Idaho, Moscow, Idaho 83843, USA*

In this study the material damping of laminated composites is derived analytically. The derivation is based on the classical lamination theory in which there are eighteen material constants in the constitutive equations of laminated composites. Six of them are the extensional stiffnesses designated by $[A]$ six of them are the coupling stiffnesses designated by $[B]$ and the remaining six are the flexural stiffnesses designated by $[D]$. The derivation of damping of $[A]$, $[B]$ and $[D]$ is achieved by first expressing $[A]$, $[B]$ and $[D]$ in terms of the stiffness matrix $[Q]^{(k)}$ and $h_k$ of each lamina and then using the relations of $Q_{ij}^{(k)}$ in terms of the four basic engineering constants $E_L$, $E_T$, $G_{LT}$ and $\nu_{LT}$. Next we apply elastic and viscoelastic correspondence principle by replacing $E_L$, $E_T$ . . . by the corresponding complex modulus $E_L^*$, $E_T^*$, . . . , and $[A]$ by $[A]^*$, $[B]$ by $[B]^*$ and $[D]$ by $[D]^*$ and then equate the real parts and the imaginary parts respectively. Thus we have expressed $A'_{ij}$, $A''_{ij}$, $B'_{ij}$, $B''_{ij}$ and $D'_{ij}$, $D''_{ij}$ in terms of the material damping $\eta_L^{(k)}$ and $\eta_T^{(k)}$ . . . of each lamina. The damping $\eta_L^{(k)}$, $\eta_T^{(k)}$ . . . have been derived analytically by the authors in their earlier publications. Numerical results of extensional damping ${}_I\eta_{ij} = A''_{ij}/A'_{ij}$ coupling damping ${}_C\eta_{ij} = B''_{ij}/B'_{ij}$ and flexural damping ${}_F\eta_{ij} = D''_{ij}/D'_{ij}$ are presented as functions of a number of parameters such as fibre aspect ratio $l/d$, fibre orientation $\theta$, and stacking sequence of the laminate.

## 1. Introduction

Damping is a kind of energy dissipation. For fibre reinforced composites, damping may be primarily due to one or a combination of the following mechanisms

(a) viscoelastic behaviour of matrix and/or fibres
(b) thermoelastic damping due to cyclic heat flow
(c) coulomb friction due to slip in unbonded regions of the fibre–matrix interface.
(d) dissipation caused by microscopic or macroscopic damage in the composite.

The first two mechanisms are the basic causes of damping for undamaged composites. The objective of this research is to determine analytically the damping of laminated polymer matrix composites.

During the past two years, the authors have engaged in research in damping for composite materials both analytically and experimentally. During the course of research we have successfully developed analytical methods to predict internal material damping for unidirectional composites [1], unidirectional off-axis composites [2, 3] and randomly oriented short-fibre composites [4, 5].

There are two analytical methods which have been employed by the authors. The first method is to use the force-balance approach in conjunction with Cox's shear-lag analysis [6] to derive the expression for the elastic modulus $E_L$ along the fibre direction of unidirectional aligned short-fibre composites. Then the elastic-viscoelastic correspondence principle is used to obtain the expression for the complex modulus $E_L^*$. The complex equation for $E_L^*$ then becomes two real equations for storage and loss moduli. The material damping is obtained as the ratio of the loss modulus to the storage modulus.

The second method is the energy approach. In this approach the energy stored in the fibre and matrix, and energy dissipated due to interfacial shear stresses, are used to find the values of storage as well as loss moduli.

By using these approaches, we have obtained numerical results for damping of unidirectional aligned short-fibre composites, unidirectional off-axis short-fibre composites and also randomly oriented short-fibre composites. Important parameters which will affect damping are also identified as stiffness ratio $E_f/E_m$, fibre volume fraction $V_f$, loading angle $\theta$, fibre aspect ratio $l/d$ and damping of the fibre and matrix materials $\eta_f$ and $\eta_m$.

In this paper the internal material damping of laminated composites is studied analytically. In this study, the force-balance approach is used. In the force-balance approach we apply the classical lamination theory to obtain the $[A]$, $[B]$ and $[D]$ stiffness matrices [7]. Damping in laminated composites can therefore be classified as in-plane damping which is defined as the ratio of $A_{ij}$ loss to $A_{ij}$ storage, i.e. $A''_{ij}/A'_{ij}$ coupled damping defined as $B_{ij}$ loss to $B_{ij}$ storage, i.e. $B''_{ij}/B'_{ij}$ and flexural damping defined as the ratio of $D_{ij}$ loss to $D_{ij}$ storage, i.e. $D''_{ij}/D'_{ij}$ $(i, j = 1, 2, 6)$. $A_{ij}$, $B_{ij}$, and $D_{ij}$ are


0022–2461/87 $03.00 + .12 

functions of $\bar{Q}_{ij}^{(k)}$ of each lamina which are in turn functions of the four basic engineering material constants $E_L$, $E_T$, $G_{LT}$ and $\nu_{LT}$ and the angle $\theta$. Therefore, the material damping of laminated composites can be obtained from the definition of $A_{ij}$, $B_{ij}$ and $D_{ij}$ and the elastic-viscoelastic correspondence principle in the following form

$$A_{ij}^* = A'_{ij} + iA''_{ij} = \sum_{k=1}^{N} (\bar{Q}'_{ij} + i\bar{Q}''_{ij})^{(k)}(h_k - h_{k-1})$$

$$B_{ij}^* = B'_{ij} + iB''_{ij} = \frac{1}{2}\sum_{k=1}^{N} (\bar{Q}'_{ij} + i\bar{Q}''_{ij})^{(k)}(h_k^2 - h_{k-1}^2)$$

$$D_{ij}^* = D'_{ij} + iD''_{ij} = \frac{1}{3}\sum_{k=1}^{N} (\bar{Q}'_{ij} + i\bar{Q}''_{ij})^{(k)}(h_k^3 - h_{k-1}^3) \quad (1)$$

where $i = \sqrt{-1}$ and both $Q'_{ij}$ and $Q''_{ij}$, are functions of $E'_L$, $E'_T$, $G'_{LT}$, $E''_L$, $E''_T$ and $G''_{LT}$. The expressions for $E'_L$, $E''_L$, $E''_T$, $E'_T$, $G'_{LT}$ and $G''_{LT}$ have been derived in [2, 3] by the authors.

The material damping in laminated composites is therefore expressed as

$$
\begin{aligned}
{}_{I}\eta_{ij}^{(\text{in-plane})} &= A''_{ij}/A'_{ij} \\
{}_{c}\eta_{ij}^{(\text{coupled})} &= B''_{ij}/B'_{ij} \qquad (i, j = 1, 2, 6) \qquad (2) \\
{}_{F}\eta_{ij}^{(\text{flexural})} &= D''_{ij}/D'_{ij}
\end{aligned}
$$

where $A''_{ij}$, $A'_{ij}$, $B''_{ij}$, $B'_{ij}$, $D''_{ij}$ and $D'_{ij}$ are defined in Equation 1 in terms of $Q'^{(k)}_{ij}$, $Q''^{(k)}_{ij}$ and the position $h_k$ relative to the mid-surface. For symmetric laminates $B_{ij} = 0$ and ${}_{c}\eta_{ij}^{(\text{coupled})}$ also vanish.

## 2. Analysis

The relations between $Q_{ij}$ $(i, j = 1, 2, 6)$ and the four basic engineering constants are given by the well-known formulae

$$
\begin{aligned}
Q_{11} &= \frac{E_L}{1 - (\nu_{LT})^2 E_T/E_L} \\
Q_{12} &= \frac{\nu_{LT} E_T}{1 - (\nu_{LT})^2 E_T/E_L} \qquad (3) \\
Q_{22} &= \frac{E_T}{1 - (\nu_{LT})^2 E_T E_L} \\
Q_{66} &= G_{LT}
\end{aligned}
$$

where

$$E_L = E_f V_f (1 + R)\left[1 - \frac{\text{Tanh}(\beta l/2)}{\beta l/2}\right] + E_m(V_m - V_f R) \quad (4)$$

and $R$ is the fibre tip spacing/fibre length (see Fig. 1)

$$\beta_L = 4l/d\left(\frac{G_m}{E_f}\frac{1}{\ln \pi/4V_f}\right) \quad (5)$$

$$E_T = E_m \frac{1 + 2\eta_1 V_f}{1 - \eta_1 V_f} \quad (6)$$

$$G_{LT} = G_m \frac{1 + \eta_2 V_f}{1 - \eta_2 V_f} \quad (7)$$

$$\nu_{LT} = \nu_f V_f + \nu_m V_m \quad (8)$$

$$\eta_1 = \frac{E_f/E_m - 1}{E_f/E_m + 2} \quad (9)$$

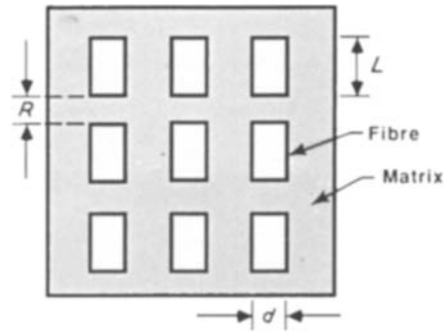


*Figure 1* Aligned short fibre composites.

$$\eta_2 = \frac{G_f/G_m - 1}{G_f/G_m + 1} \quad (10)$$

Equations 4 and 5 are obtained from Cox's shear lag model [6] and Equations 6 and 7 are well-known Halpin-Tsai equations. If we consider both fibre and matrix materials are viscoelastic materials, then in Equations 4 through 8 we have to replace $E_L$ by $E_L^*$, $E_f$ by $E_f^*$ i.e.

$$
\begin{aligned}
E_L^* &= E_L(1 + i\eta_L) \\
&= E_f(1 + i\eta_f)V_f R\left[1 - \frac{\tanh \beta^* l/2}{\beta^* l/2}\right] \\
&\quad + E_m(1 + i\eta_m)(V_m - V_f R) \qquad (11)
\end{aligned}
$$

$$\beta^* L = \beta' L + i\beta''_L = 4L/d\,\frac{G_m(1 + i\eta_{mG})}{E_f(1 + i\eta_f)}\,\frac{1}{\ln \pi/4V_f} \quad (12)$$

$$E_T(1 + i\eta_T) = E_m(1 + i\eta_m)\frac{1 + 2\eta_1^* V_f}{1 - \eta_1^* V_f} \quad (13)$$

$$G_{LT}(1 + i\eta_{LT}) = G_m(1 + i\eta_{mG})\frac{1 + \eta_2^* V_f}{1 - \eta_2^* V_f} \quad (14)$$

$$\nu_{LT}(1 + i\eta_{\nu_{LT}}) = \nu_f(1 + i\eta_{\nu_f})V_f + \nu_m(1 + i\eta_{\nu_m})V_m \quad (15)$$

Upon separation of real and imaginary parts in Equations 11 through 15 and equating the real parts and the imaginary parts respectively we can derive the damping coefficients $\eta_L$, $\eta_T$, $\eta_{GLT}$, and $\eta_{\nu_{LT}}$, i.e. damping along the longitudinal direction, damping along the transverse direction, shear damping and damping of Poisson's ratio for the unidirectional composites in terms of $E_f/E_m$, $G_f/G_m$, $\eta_f$, $\eta_m$, fibre aspect ratio $l/d$, fibre tip spacing $R$, fibre volume fraction $V_f$ and fibre orientation angle $\theta$. The expressions of $\eta_T$, $\eta_{GLT}$ can be found in the authors earlier publications [1–3]. The derivation of the real and imaginary parts of the Poisson's ratio was based on observation by Gibson and Plunkett [8] that the bulk modulus $K$ is independent of frequency. With this observation, for isotropic fibre and matrix materials we can easily derive the real part and the imaginary part of the Poisson's ratio respectively with the result

$$
\begin{aligned}
\nu' &= 1/2\left(1 - \frac{E'}{3K}\right) \\
\nu'' &= -1/2\,\frac{E''}{3K} \qquad (16)
\end{aligned}
$$

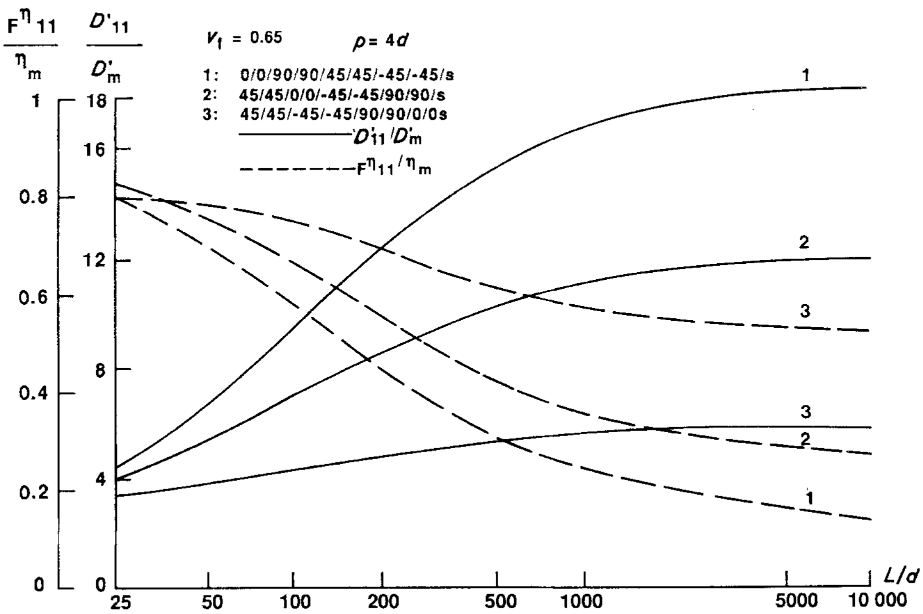


*Figure 2* Plots of $D'_{11}/D_m$ and ${}_F\eta_{11}/\eta_m$ against $L/d$ for quasi-isotropic graphite epoxy composites.

Substitution of Equations 12 through 15 yields the expressions of

$$
\begin{aligned}
Q^*_{11} &= Q'_{11} + iQ''_{11} \\
Q^*_{22} &= Q'_{22} + iQ''_{22} \\
Q^*_{12} &= Q'_{12} + iQ''_{12} \\
Q^*_{66} &= G^*_{LT} = G_{LT}(1 + i\eta_{GLT})
\end{aligned}
\qquad (17)
$$

in terms of $E_f/E_m$, $\eta_f$, $\eta_m$, $V_f$, $l/d$ and $R$. The detail expressions $Q'_{11}, \ldots Q''_{66}$ are too lengthy to be presented in this paper, but the derivation is straight forward.

Since $[A]$, $[B]$ and $[D]$ are functions of $\bar{Q}'_{ij}$ and $\bar{Q}''_{ij}$ $(i, j = 1, 2, 6)$ which are related to $Q_{ij}$ by the following relations [7]

$$
\begin{aligned}
\bar{Q}_{11} &= Q_{11}\cos^4\theta + Q_{22}\sin^4\theta \\
&\quad + 2(Q_{12} + 2Q_{66})\sin^2\theta\cos^2\theta \\
&\vdots \\
\bar{Q}_{26} &= (Q_{11} - Q_{12} - 2Q_{66})\cos\theta\sin^3\theta \\
&\quad - (Q_{22} - Q_{12} - 2Q_{66})\cos^3\theta\sin\theta
\end{aligned}
\qquad (18)
$$

the expressions of

$$
\begin{aligned}
A^*_{ij} &= A_{ij}(1 + i_I\eta_{ij}) \\
\beta^*_{ij} &= \beta_{ij}(1 + i_c\eta_{ij}) \qquad (i, j = 1, 2, 6) \quad (19) \\
D^*_{ij} &= D_{ij}(1 + i_F\eta_{ij})
\end{aligned}
$$

can be derived from Equations 1, 3 and 4 through 16. Again the expressions are too lengthy to be given here. Numerical results of $A^*_{11}$, $A^*_{66}$, $D^*_{11}$ and $D^*_{66}$ are presented in the next section as functions of the stacking sequence, fibre aspect ratio $l/d$, fibre tip spacing $R$ and fibre volume fraction $V_f$.

## 3. Numerical results

The important quantities to be presented are:

${}_I\eta_{11}$ = extensional damping along the direction 1
$E'_{11}$ = extensional storage modulus along direction 1
${}_I\eta_{66}$ = in plane shear damping
$E'_{66}$ = in plane shear storage modulus
${}_F\eta_{11}$ = flexural damping about the axis 1
$D'_{11}$ = flexural storage modulus along direction 1
${}_F\eta_{66}$ = flexural shear damping
$D'_{66}$ = fluxural shear storage modulus

Numerical results of the above quantities are presented in Figs 2 to 11 in normalized nondimensional form.

In Figs 2 and 3 ${}_F\eta_{11}$, $D'_{11}$, ${}_F\eta_{66}$ and $D'_{66}$ of quasi-isotropic graphite–epoxy composites are plotted as a function of the fibre aspect ratio $l/d$. Four different stacking sequences are included. The results are not surprising. Under flexural loading, the bending stiffness $D'_{11}$ is the highest when 0° ply is placed on the top and bottom surfaces of the laminate and becomes the lowest when 0° ply is located in the midsurface of the laminate. For $D'_{66}$ the situation is just the opposite. It is maximum for a given $l/d$ for the laminate with $\pm 45°$ plies on the top and bottom and is minimum with $\pm 45°$ plies on the midsurface. The behaviour of damping is just opposite to the corresponding stiffness. This observation is clearly indicated in Figs 2 and 3, i.e. $D'_{11}$ and $D'_{66}$ increase as $l/d$ increases and ${}_F\eta_{11}$ and ${}_F\eta_{66}$ decrease as $l/d$ increases.

Figs 4 to 7, show the four in-plane extensional properties i.e. $E'_{11}$, ${}_I\eta_{11}$, $E'_{66}$ and ${}_I\eta_{66}$ of angle-ply graphite–epoxy as a function of the ply angle $\theta$. Maximum $E'_{11}$ occurs at 0° and drops sharply as $\theta$ increases and reaches to the same value as $\theta = 90°$ for all value of $l/d$. This is true since when $\theta = 90°$, $E'_{11}$ approaches to $E'_T$ which is assumed to be independent of the fibre aspect ratio $l/d$. The maximum value of ${}_I\eta_{11}$ depends on the stacking sequence. This observation was also noticed in the authors previous publications [2, 3] for unidirectional composites. Again at $\theta = 90°$, ${}_I\eta_{11}$ reaches the same value regardless of the value of $l/d$.

$E'_{66}$ and ${}_I\eta_{66}$ behave just the opposite with the exception that both plots are symmetric with respect to the vertical line of $\theta = 45°$. Maximum $E'_{66}$ occurs at $\theta = 45°$ and larger fibre aspect ratio and maximum

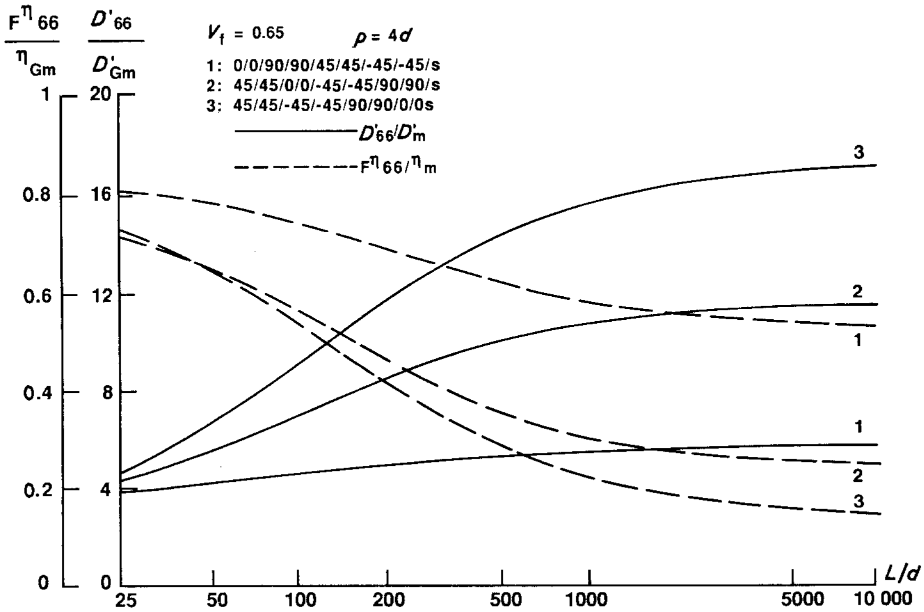


*Figure 3* Plots of $D'_{66}/D_{Gm}$ and $_{F}\eta_{66}/\eta_{Gm}$ against $L/d$ for quasi-isotropic graphite epoxy composites.

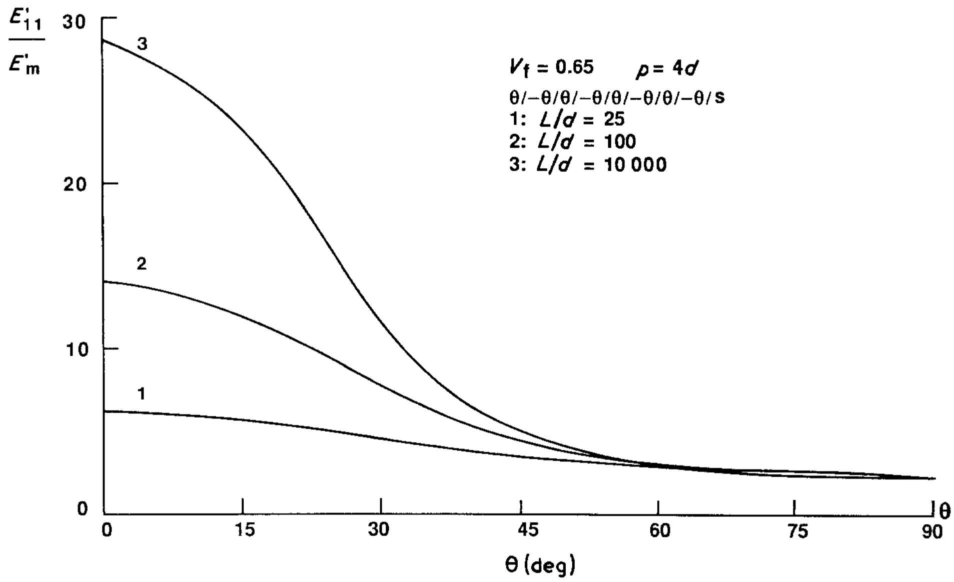


*Figure 4* Plots of $E'_{11}/E'_m$ against $\theta$ using $L/d$ as a parameter for angle ply graphite epoxy composites.

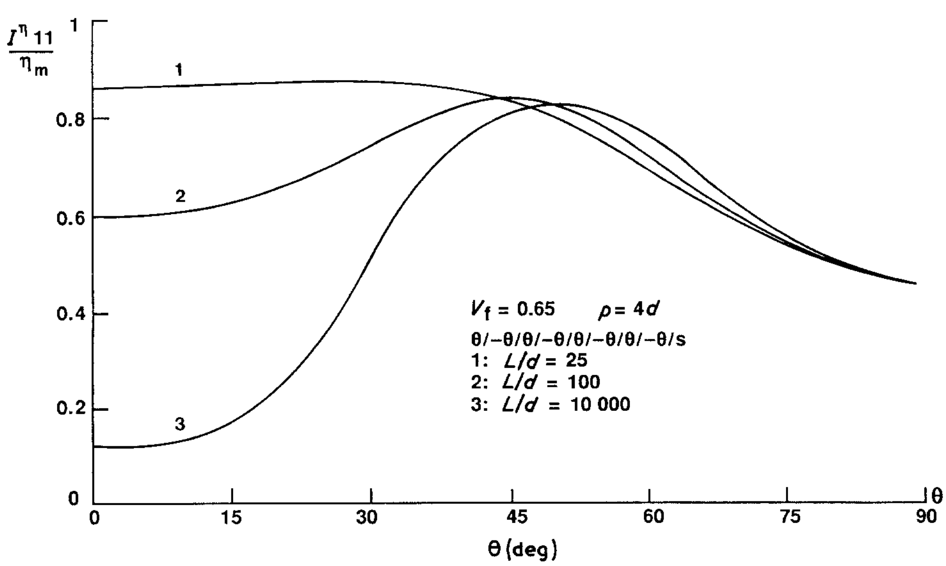


*Figure 5* Plots of $_{I}\eta_{11}/\eta_m$ against $\theta$ using $L/d$ as a parameter for angle ply graphite epoxy composites.

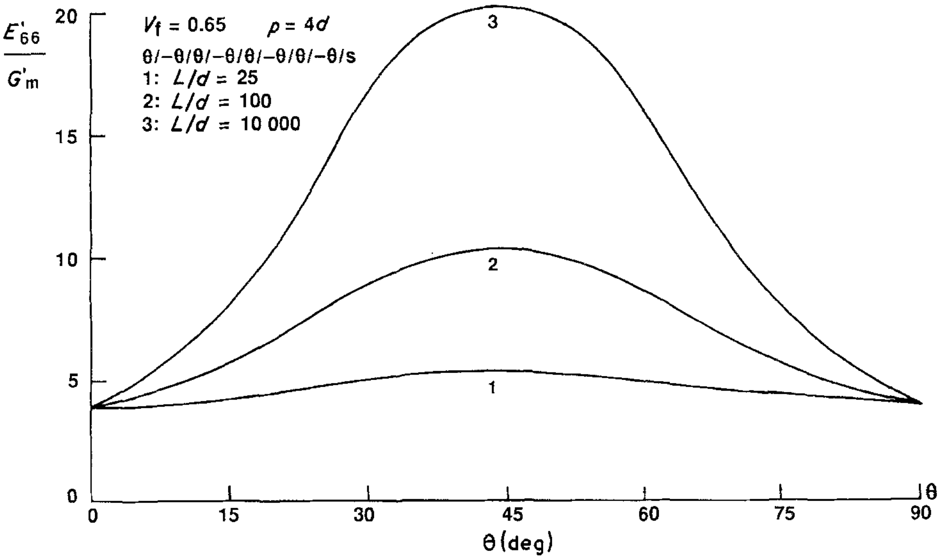


*Figure 6* Plots of $E'_{66}/G'_{m}$ against $\theta$ using $L/d$ as a parameter for angle ply graphite epoxy composites.

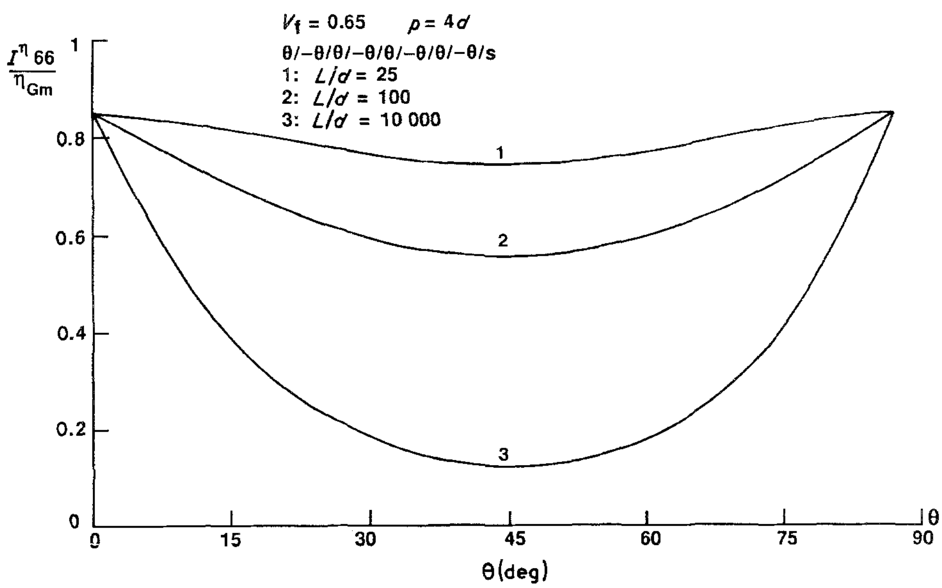


*Figure 7* Plots of ${}_{I}\eta_{66}/\eta_{Gm}$ against $\theta$ using $L/d$ as a parameter for angle ply graphite epoxy composites.

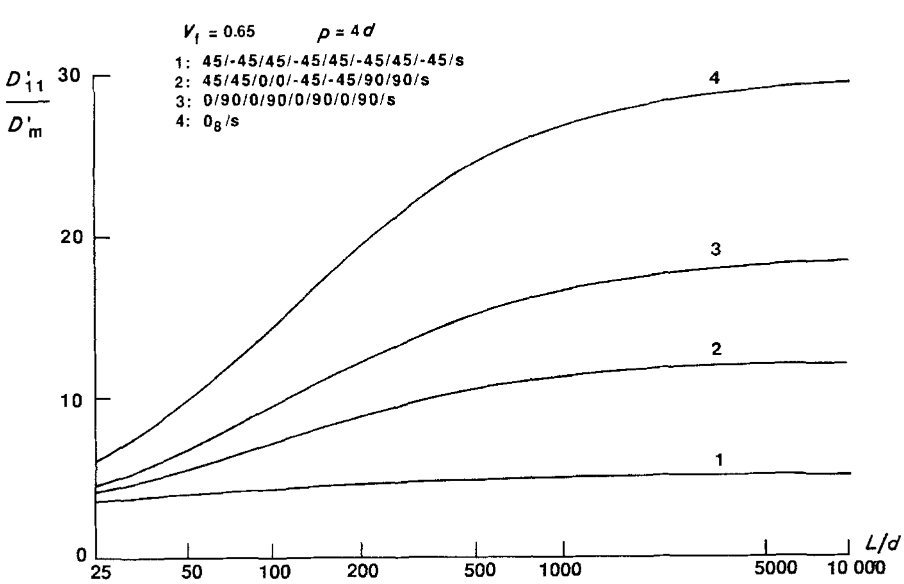


*Figure 8* Comparisons of $D'_{11}/D'_{m}$ against $L/d$ for four kinds of laminated graphite epoxy composites.

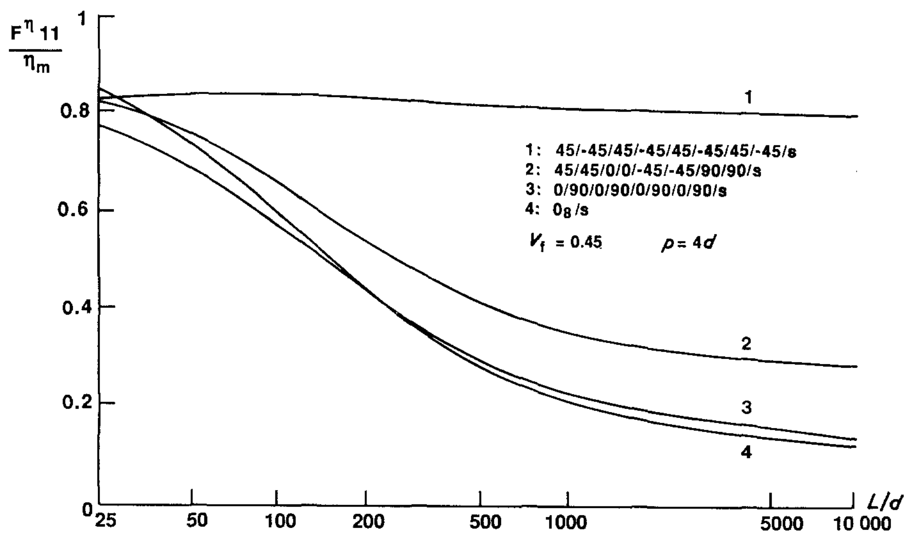


*Figure 9* Comparison of $_F\eta_{11}/\eta_m$ against $L/d$ for four kinds of laminated graphite epoxy composites.

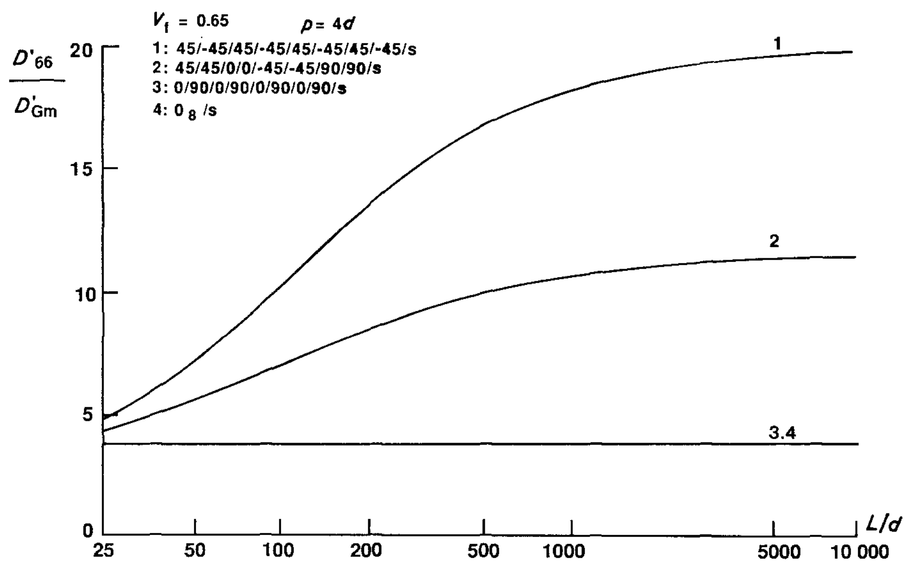


*Figure 10* Comparisons of $D'_{66}/D'_{Gm}$ against $L/d$ for four kinds of laminated graphite epoxy composites.

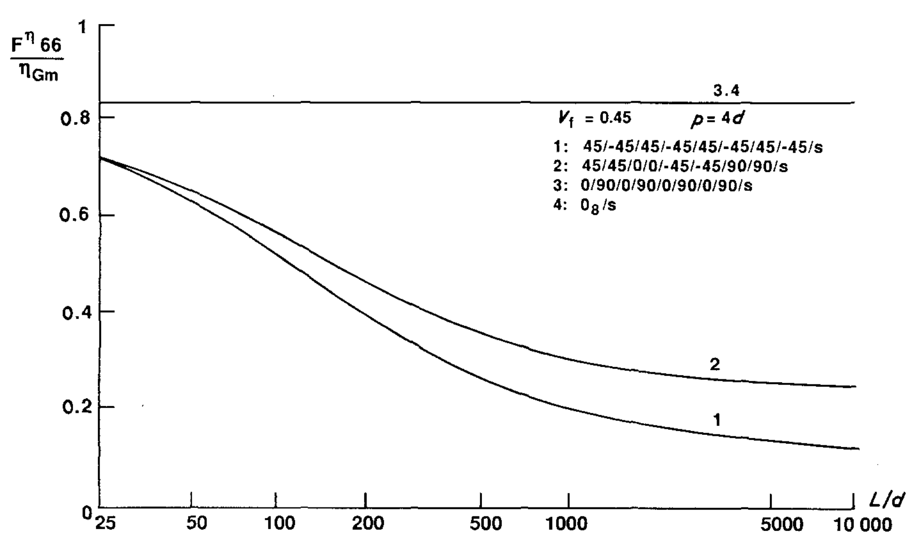


*Figure 11* Comparison of $_F\eta_{66}/\eta_{Gm}$ against $L/d$ for four kinds of laminated graphite epoxy composites.

$_I\eta_{66}$ also occurs at $\theta = 45°$ but smaller fibre aspect ratio.

Figs 8 to 11, show plot of $D'_{11}$, $_F\eta_{11}$, $D'_{66}$ and $_F\eta_{66}$ of laminated graphite–epoxy composites with four different stacking sequences as a function of $l/d$. No surprising results were observed. The trend is always the same, i.e. materials with higher damping will have lower stiffness and vice versa. For instance $0_8$ laminate has maximum $D'_{11}$ and minimum $D'_{66}$ and $[45/\text{-}45/45/\text{-}45]_{2S}$ laminate has maximum $D'_{66}$ and minimum $D'_{11}$. But for dampings, i.e. for $_F\eta_{11}$ and $_F\eta_{66}$ these trends are just reversed.

## 4. Concluding remarks

Analytical prediction of extensional stiffness and damping in-plane shear stiffness and damping, flexural stiffness and damping and flexural shear stiffness and damping of laminated composites were obtained from the classical theory of lamination along with the elastic-viscoelastic correspondence principle and separation of the real and imaginary parts. Numerical results for laminated composites indicate similar trends as observed in the unidirectional composites, i.e. damping and stiffness always behave in opposite manners. Designers, thus, should make some compromise in order to achieve optimum performance of composite structures.

Finally the above analysis does not take into account the contribution of the interlaminar stresses. A three-dimensional model by using the finite-element approach include the influences of interlaminar stresses has been developed and the results will be published in the near future.

## Acknowledgement

The authors gratefully acknowledge support of this research work from AFOSR under Grant No. AFOSR-83-0154 and AFOSR-83-0156 monitored by Dr D. R. Ulrich, program manager, Directorate of Chemical and Atmospheric Sciences AFOSR Bolling Air Force Base, Washington, DC.

## References

1. R. F. GIBSON, S. K. CHATURVEDI and C. T. SUN, *J. Mater. Sci.* **17** (1982) 3499.
2. C. T. SUN, S. K. CHATURVEDI and R. F. GIBSON, Computers and Structures **20** (1985) 391.
3. C. T. SUN, R. F. GIBSON and S. K. CHATURVEDI, *J. Mater. Sci.* **20** (1985) 2575.
4. C. T. SUN, J. K. WU and R. F. GIBSON, *J. Reinforced Plastics and Composites* **4** (1985) 262.
5. S. A. SUAVEZ, R. F. GIBSON, C. T. SUN and S. K. CHATURVEDI, "The Influence of Fiber Length and Fiber Orientation of Damping and Stiffness of Polymer Composite Materials", presented at the SESA Spring 1985 Conference, June 9–13, 1985, Las Vegas, Nevada. In "Experimental Mechanics" Vol. 26 (1986) p. 175.
6. H. L. COX, *Brit. J. Appl. Phys.* **3** (1953) 72.
7. B. D. AGARWAL and L. J. BROUTMAN, "Analysis and Performance of Fiber Composites", (John-Wiley Interscience, New York, 1979).
8. R. F. GIBSON and R. PLUNKETT, *J. Composite Mater.* **10** (1976) 325.

*Received 15 April*
*and accepted 30 June 1986*